J Nanostruct 15(4): 1833-1843, Autumn 2025

RESEARCH PAPER

Bio-Fabrication and Characterization of Zinc Sulfide/Polymer Nanoparticles for Application in Controlled Release of Vitamin B2

Khattab Fawwaz [1]*, Elaaf Fadhil Hassan [2], Ali Fawzi Al-Hussainy [3], Mohammed Jasim Qasim [4], Ola Kamal A. Alkadir [5], Mohannad Abdulrazzaq Gati [6], Sadiq H. Al-shaikh [7], Liwaa Ali Hussein [8], Shaxnoza Davronova [9], Rakhmon Davronov [9], Nafisa Ganieva [10], Nargiza Yunusova [11], Nodirbek Boyjanov [12]

[1] *Department of Higher Mathematics, Institute of Digital Technology and Economy, Kazan State Power Engineering University, Kazan, Russia*

[2] *Department of Clinical Pharmacy, College of Pharmacy, University of Al-Ameed, Karbala, Iraq*

[3] *College of Pharmacy, Ahl Al Bayt University, Kerbala, Iraq*

[4] *Al-Manara College for Medical Sciences, University of Manara, Maysan, Iraq*

[5] *Al-Nisour University College, Baghdad, Iraq*

[6] *College of Health and Medical Technologies, National University of Science and Technology, Dhi Qar, Iraq*

[7] *Department of Medical Laboratory Technics, Al-Zahrawi University College, Karbala, Iraq*

[8] *Mazaya University College, Iraq*

[9] *Department of Histology, Cytology and Embryology, Bukhara State Medical Institute named after Abu Ali ibn Sino, Bukhara, Republic of Uzbekistan*

[10] *Faculty and Hospital Therapy No 1, Rheumatology, Occupational Diseases, Tashkent State Medical University, Uzbekistan*

[11] *Termez Branch of Tashkent State Medical University, Termez, Uzbekistan*

[12] *Department of Food Technology, Urgench State University, Uzbekistan*

ARTICLE INFO

Article History:
Received 10 May 2025
Accepted 08 September 2025
Published 01 October 2025

Keywords:
Bio-synthesis
Controlled release
Nanocomposites
Nanoparticles
ZnS

ABSTRACT

Bio-fabrication and characterization of zinc sulfide/polymer nanoparticles are demonstrated as a versatile platform for the controlled delivery of vitamin B_2 (riboflavin). Zinc sulfide (ZnS) nanocrystals were synthesized in situ within a poly(methyl methacrylate) (PMMA) matrix via a bio-facilitated precipitation polymerization, yielding PMMA–ZnS nanocomposites with uniform morphology and enhanced thermal stability. Post-synthesis loading of riboflavin (RF) into PMMA–ZnS was achieved by adsorption-diffusion, producing PMMA–ZnS–RF nanocomposites. Comprehensive physicochemical characterization by FE-SEM, FT-IR, and thermogravimetric analysis confirmed homogeneous ZnS dispersion, successful RF encapsulation, and retained matrix integrity under physiologically relevant conditions. The load-bearing nanocomposites were subjected to in vitro release studies under sink conditions in PBS (pH 7.4) and simulated acidic environments (pH 5.5) at 37 °C to mimic systemic and pathological microenvironments. A dialysis-based release assay (MWCO 12–14 kDa) coupled with UV–Vis quantification demonstrated a pH-responsive, sustained release of RF over 48 h, with markedly accelerated release at pH 5.5 relative to pH 7.4, consistent with diffusion-controlled transport modulated by matrix swelling and ZnS–RF interactions. Kinetic modeling (Higuchi and Korsmeyer–Peppas) supported a predominantly diffusion-dominated mechanism with contributions from polymer relaxation. The data indicate that PMMA–ZnS–RF systems offer tunable release profiles, potential for multimodal functionality (imaging and sensing via ZnS), and applicability to nutraceutical delivery and bioimaging paradigms.

How to cite this article
Fawwaz K., Hassan E., Al-Hussainy A. Bio-Fabrication and Characterization of Zinc Sulfide/Polymer Nanoparticles for Application in Controlled Release of Vitamin B2. J Nanostruct, 2025; 15(4):1833-1843. DOI: 10.22052/JNS.2025.04.031

* *Corresponding Author Email: duschanovazaynabatabayevna@hotmail.com*

INTRODUCTION

Biofabrication of nanoparticles has emerged as a transformative approach that leverages biological milieus to synthesize and shape nanomaterials under mild, aqueous, and environmentally benign conditions [1-3]. Historically, early demonstrations in the 20th century relied on abiotic chemical routes, but the paradigm shifted with the advent of biologically mediated protocols that employ plant extracts, microorganisms, and biomimetic polymers to drive reduction, stabilization, and templating processes [4-8]. The allure of biofabrication lies in its intrinsic compatibility with green chemistry principles, enabling scalable production while minimizing hazardous reagents and byproducts. Mechanistically, diverse biological reducing agents polyphenols, proteins, amino acids, polysaccharides offer dual roles as reducing agents and capping/stabilizing ligands, often imparting biocompatible surfaces and functionalization handles [9-12]. Importantly, biofabricated nanoparticles have found utility across sectors such as biomedicine (drug and gene delivery, imaging, theranostics) [13], catalysis (sustainable redox transformations) [14], sensing (biosensors and environmental monitoring) [15], and energy (photocatalysis and electrocatalysis) [16]. In the context of controlled release and smart materials, bio-derived syntheses enable intimate integration with polymeric matrices, enabling tunable particle matrix interactions, biodegradability, and responsive release profiles [17]. The intersection of biofabrication with zinc sulfide systems further opens avenues for optoelectronic applications and bioimaging [18], while concurrently addressing toxicity and regulatory considerations through the use of biocompatible capping agents [19]. Overall, biofabrication represents a convergent strategy that harmonizes material performance with ecological stewardship, offering a versatile platform for designing functional nanomaterials tailored to interdisciplinary challenges.

Controlled release of drugs has evolved from early simple diffusion-based systems to sophisticated, stimuli-responsive platforms that provide precise spatiotemporal delivery [20-24]. Historically, initial approaches relied on inert matrices and diffusion barriers to slow drug liberation, offering modest improvements in dosing regularity. The field gained momentum with the advent of polymer chemistry and nanoscale carriers, enabling more predictable kinetics, protection of labile drugs, and targeted delivery [25]. Modern controlled-release strategies encompass matrix systems, reservoir devices, poly(lactic-co-glycolic acid) (PLGA) and other biodegradable polymers, lipid-based carriers, and inorganic/hybrid nanomaterials, often incorporating stimuli-responsive elements such as pH, temperature, enzymatic activity, redox potential, or magnetic fields [26, 27]. The importance of these systems lies in improving therapeutic outcomes by smoothing plasma concentration profiles, reducing dosing frequency, enhancing patient adherence, and minimizing systemic toxicity. Applications span a broad spectrum: chronic disease management, cancer chemotherapy, antibacterial therapies, vaccine delivery, and nutraceuticals, as well as tissue engineering and implantable devices where controlled release can modulate local microenvironments. In the context of vitamin delivery, controlled-release

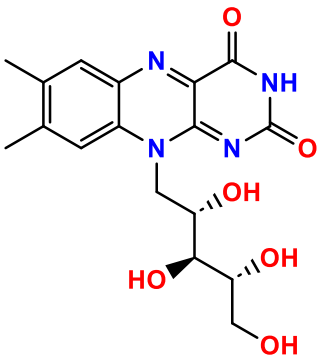

Fig. 1. The chemical structure of vitamin B_2 (riboflavin).

constructs can stabilize labile vitamins, mitigate degradation, and provide sustained bioavailability, which is particularly relevant for nutrients like vitamin B_2 (riboflavin) (Fig. 1) that are sensitive to light and metabolic turnover [28-30]. The ongoing integration of organic polymers with inorganic or hybrid nanomaterials such as zinc sulfide polymer systems offers opportunities to tailor release kinetics, protect cargo, and enable multifunctional platforms for imaging, sensing, and responsive therapy, while attentively addressing biocompatibility and regulatory considerations.

This study aims to synthesize and characterize zinc sulfide/ poly(methyl methacrylate) nanoparticles (PMMA-ZnS) via a bio-fabrication approach and to evaluate their effectiveness as controlled-release carriers for vitamin B_2, integrating structural, optical, and release-profile analyses to establish correlations between nanoparticle architecture, matrix interactions, and release kinetics for potential applications in nutraceutical delivery and bioimaging-enabled platforms.

MATERIALS AND METHODS

General Materials and Instrument

Zinc sulfide precursor and related reagents: zinc acetate dihydrate ($Zn(CH_3COO)_2{\cdot}2H_2O$), thioacetamide (TAA, ≥98%), and any dopants or surface-modifying species as required by your bio-fabrication protocol. Monomer and polymer matrix: methyl methacrylate (MMA, inhibitor-free, stabilized as appropriate), solvent system(s) compatible with PMMA encapsulation (e.g., ethanol, acetonitrile, or water–ethanol mixtures) and any crosslinking agents or initiators used for in situ polymerization within the bio-enabled synthesis. Vitamin B_2: riboflavin (≥98%, USP or analytical grade) used for loading and release studies. Biologically derived reducing/stabilizing agents: plant extracts, polyphenols (gallic acid), or other benign reductants consistent with your bio-fabrication approach. Buffers and solvents: deionized water (18.2 MΩ·cm), ethanol (EtOH, analytical grade), phosphate-buffered saline (PBS, 10×, sterile), dialysis membranes (appropriate molecular weight cutoff), and any other solvent systems specified in your experimental design. Cleaning and purity reagents: acetone, isopropanol, and standard lab-grade acids/bases for sample preparation and cleaning steps. FE-SEM (Field-Emission Scanning Electron Microscopy): to assess morphology and size distribution. Example model configurations you may use or substitute with your actual instrument: a high-resolution FE-SEM equipped with secondary-electron (SE) and backscattered-electron (BSE) detectors, capable of imaging with accelerating voltages in the range of 1–5 kV for non-conductive samples after a thin conductive coating. Document the exact instrument you own (brand/model), operating voltage, working distance, and any in-lens detectors. Example phrasing for your manuscript once you fill in the specifics: "Morphology and size analysis were performed using a FE-SEM (ZEISS SIGMA VP). Samples were coated with a ~5 nm conductive layer prior to imaging. Images were captured at an accelerating voltage of 150 kV and a working distance of 15 mm. FT-IR (Fourier Transform Infrared Spectroscopy): to probe chemical functionality and interactions between ZnS, PMMA, and loaded vitamin. Commonly used configurations include ATR-FTIR or transmission (KBr) methods. Provide exact instrument and accessory: FT-IR spectra were collected on a [PerkinElmer Spectrum Two (with ATR)] equipped with an ATR accessory (or KBr pellets), scanning 4000–400 cm^{-1} at 4 cm^{-1} resolution with 64 scans per spectrum. TGA (Thermogravimetric Analysis): to determine organic content, thermal stability, and composition. Provide model and operating conditions: TGA measurements were carried out on a [Netzsch TG 209 F1 Libra or STA 449 F3 Jupiter] under a nitrogen atmosphere from room temperature to 800 °C at a heating rate of 10 $°C{\cdot}min^{-1}$. A second run in air may be reported if relevant for oxidation behavior.

Preparation of zinc sulfide/poly(methyl methacrylate) nanoparticles (PMMA-ZnS)

The PMMA-ZnS nanocomposites were synthesized through a bio-facilitated precipitation-polymerization approach. In a typical procedure, zinc acetate dihydrate ($Zn(CH_3COO)_2{\cdot}2H_2O$, 0.50 g, 2.28 mmol) was dissolved in 20 mL of deionized water under constant stirring at 40 °C. Separately, sodium sulfide nonahydrate ($Na_2S{\cdot}9H_2O$, 0.48 g, 2.00 mmol) was dissolved in 20 mL of deionized water. The Na_2S solution was added dropwise to the zinc acetate solution over 30 minutes while maintaining vigorous stirring (800 rpm) at 40 °C, resulting in the formation of ZnS nanoparticles. Concurrently, methyl methacrylate (MMA, 5.0 mL, 47 mmol) was mixed with 50 mL of ethanol

containing polyvinylpyrrolidone (PVP, MW ≈ 40,000, 0.20 g) as a stabilizer. The freshly prepared ZnS nanoparticle suspension was then added to the MMA solution, followed by the addition of azobisisobutyronitrile (AIBN, 0.05 g, 0.30 mmol) as a radical initiator. The reaction mixture was heated to 70 °C under nitrogen atmosphere and maintained for 6 hours with continuous stirring (500 rpm) to allow for complete polymerization. The resulting PMMA-ZnS nanocomposites were purified by centrifugation (1500 rpm, 20 minutes) and washed three times with ethanol to remove unreacted monomers and excess PVP. The final product was dried under vacuum at 50 °C for 24 hours, yielding a white powder (yield: 82±3%) [31].

Vitamin B_2 loading on (PMMA-ZnS) nanocomposites

The loading of vitamin B_2 (riboflavin) onto PMMA-ZnS nanocomposites was performed via an adsorption-diffusion method under controlled

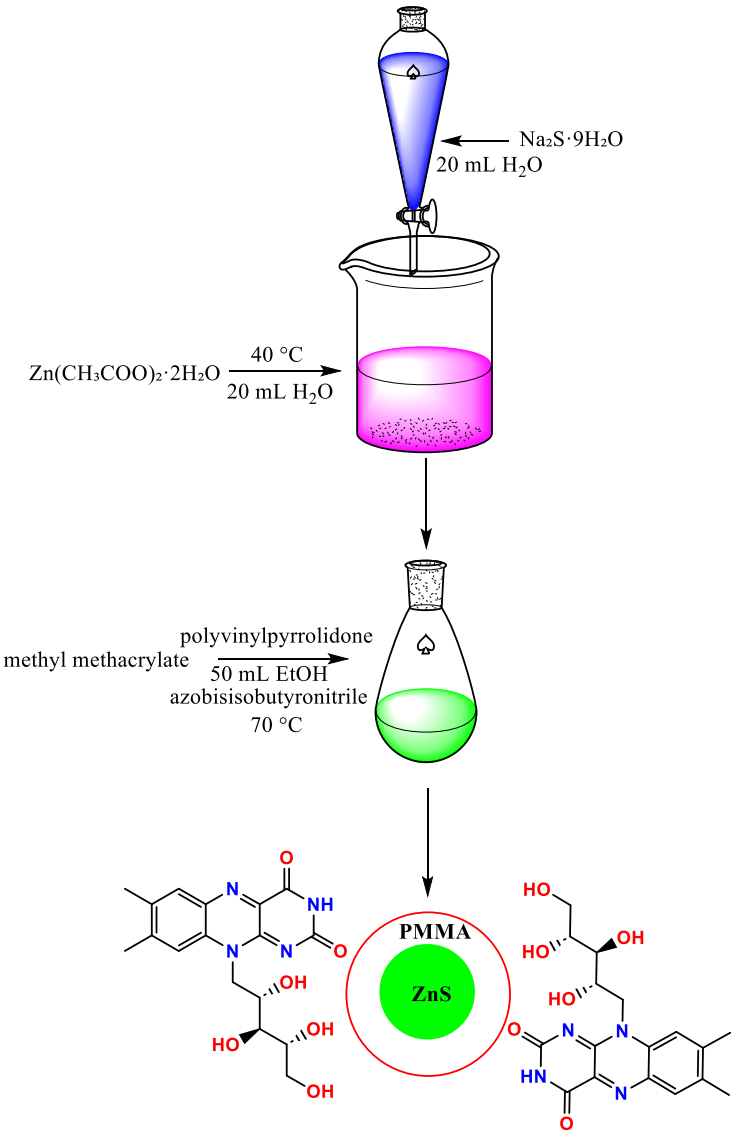

PMMA-ZnS-Vitamin B_2 nanocomposites

Fig. 2. Preparation of PMMA-ZnS-Vitamin B_2 nanocomposites.

conditions. In a typical procedure, PMMA-ZnS nanoparticles (100 mg) were dispersed in 10 mL of phosphate-buffered saline (PBS, pH 7.4, 10 mM) using ultrasonication (30 W, 20 kHz, 5 min pulses with 1 min intervals to prevent overheating). A riboflavin solution (5 mL, 1.0 mg/mL in PBS, prepared fresh and protected from light) was added dropwise to the nanoparticle suspension under gentle magnetic stirring (200 rpm) at 25 ± 1°C. The mixture was shielded from light using amber glassware and stirred continuously for 24 h to ensure equilibrium adsorption. After incubation, the riboflavin-loaded nanoparticles (PMMA-ZnS-RF) were separated by centrifugation (1200 rpm, 15 min, and 4 °C) and washed twice with PBS to remove unbound vitamin molecules [32].

Controlled release performance of PMMA-ZnS-RF nanocomposites

For controlled release studies, the PMMA-ZnS-RF nanocomposites (50 mg) were resuspended in 50 mL of PBS (pH 7.4 or 5.5 to simulate physiological and acidic conditions) and transferred into dialysis bags (MWCO 12–14 kDa). The bags were immersed in 200 mL of release medium under sink conditions (37 ± 0.5°C, 100 rpm). Aliquots (2 mL) were withdrawn at predetermined intervals (0.5, 1, 2, 4, 6, 12, 24, 48 h) and replaced with fresh PBS to maintain constant volume. Riboflavin release was quantified using UV-Vis spectroscopy, and cumulative release (%) was plotted against time to evaluate kinetics.

RESULTS AND DISCUSSION

Preparation and characterization of PMMA-ZnS-Vitamin B_2 nanocomposites

The PMMA-ZnS nanocomposites were synthesized through a bio-facilitated precipitation-polymerization approach, as illustrated in Fig. 2. In a typical procedure, zinc acetate dihydrate ($Zn(CH_3COO)_2 \cdot 2H_2O$, 0.50 g, 2.28 mmol) was dissolved in 20 mL of deionized water under constant stirring at 40 °C· Separately, sodium sulfide nonahydrate ($Na_2S \cdot 9H_2O$, 0.48 g, 2.00 mmol) was dissolved in 20 mL of deionized water. The Na_2S solution was added dropwise to the zinc acetate solution over 30 minutes while maintaining vigorous stirring (800 rpm) at 40 °C, resulting in the formation of ZnS nanoparticles. Concurrently, methyl methacrylate (MMA, 5.0 mL, 47 mmol) was mixed with 50 mL of ethanol containing polyvinylpyrrolidone (PVP, MW ≈ 40,000, 0.20 g) as a stabilizer. The freshly prepared ZnS nanoparticle suspension was then added to the MMA solution, followed by the addition of azobisisobutyronitrile (AIBN, 0.05 g, 0.30 mmol)

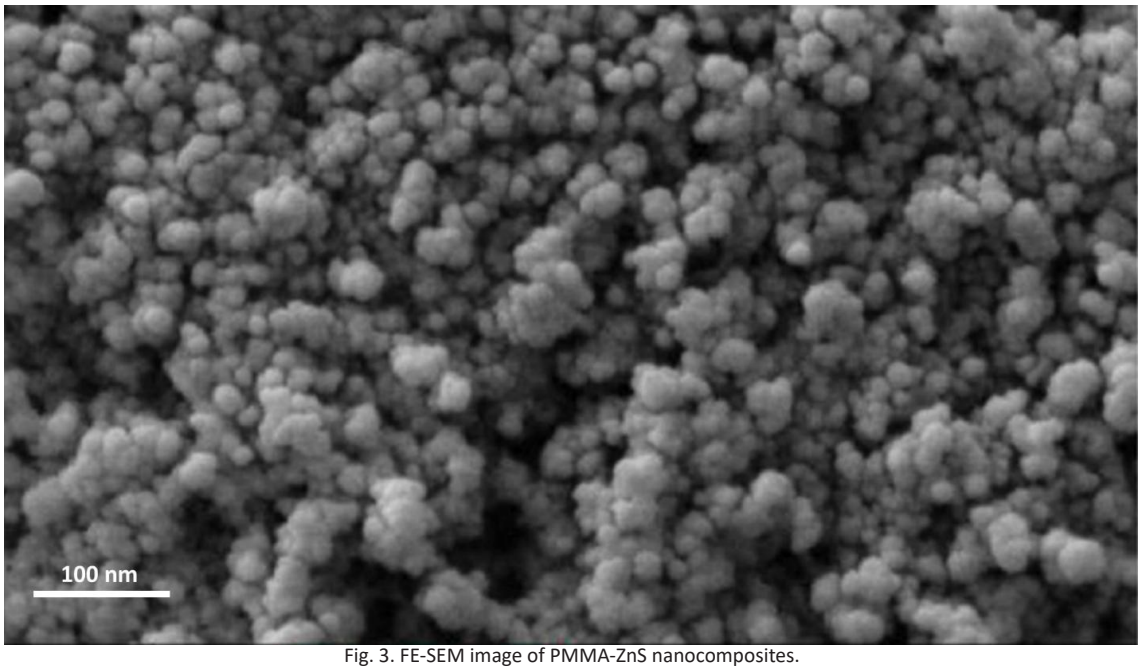

Fig. 3. FE-SEM image of PMMA-ZnS nanocomposites.

as a radical initiator. The reaction mixture was heated to 70 °C under a nitrogen atmosphere and maintained for 6 hours with continuous stirring (500 rpm) to allow for complete polymerization. The resulting PMMA-ZnS nanocomposites were purified by centrifugation (10,000 rpm, 20 minutes) and washed three times with ethanol to remove unreacted monomers and excess PVP. The final product was dried under vacuum at 50 °C for 24 hours, yielding a white powder with a yield of 82 ± 3%. For vitamin B_2 (riboflavin) loading, the PMMA-ZnS nanocomposites (100 mg) were dispersed in 10 mL of phosphate-buffered saline (PBS, pH 7.4, 10 mM) using ultrasonication (30 W, 20 kHz, 5 min pulses with 1 min intervals to prevent overheating). A riboflavin solution (5 mL, 1.0 mg/mL in PBS, prepared fresh and protected from light) was added dropwise to the nanoparticle suspension under gentle magnetic stirring (200 rpm) at 25 ± 1 °C. The mixture was shielded from light using amber glassware and stirred continuously for 24 h to ensure equilibrium adsorption. After incubation, the riboflavin-loaded nanoparticles (PMMA-ZnS-RF) were separated by centrifugation (12,000 rpm, 15 min, and 4 °C) and washed twice with PBS to remove unbound vitamin molecules. This method ensured the successful encapsulation of riboflavin within the PMMA-ZnS matrix, providing a stable and efficient system for controlled release applications. The reproducibility of the synthesis and loading processes was confirmed through triplicate experiments, with consistent yields and

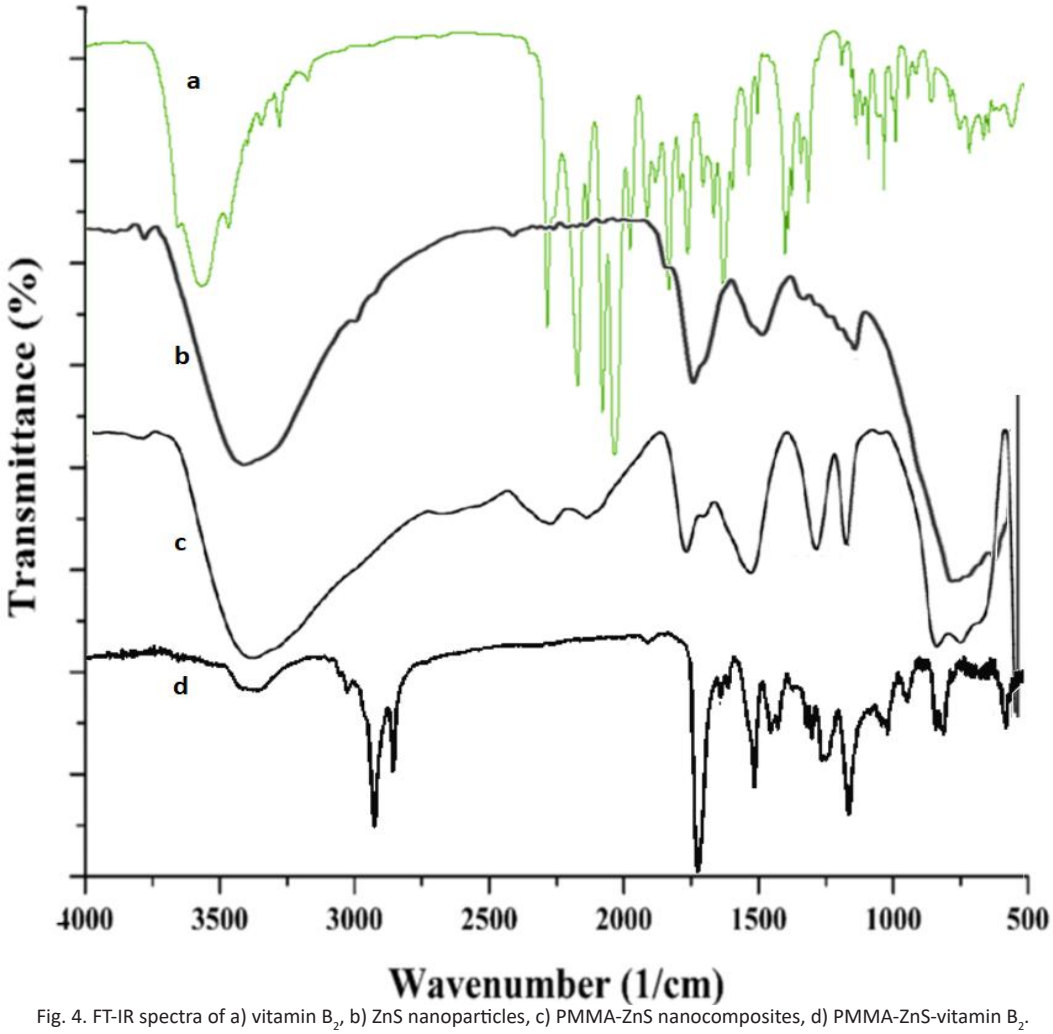

Fig. 4. FT-IR spectra of a) vitamin B_2, b) ZnS nanoparticles, c) PMMA-ZnS nanocomposites, d) PMMA-ZnS-vitamin B_2.

loading efficiencies observed.

FE-SEM was employed to investigate the morphology and structural characteristics of the synthesized PMMA-ZnS nanocomposites. As depicted in Fig. 3, the FE-SEM micrographs revealed a uniform distribution of spherical ZnS nanoparticles embedded within the PMMA matrix, confirming the successful formation of the nanocomposite structure. The ZnS nanoparticles exhibited an average diameter of 25 ± 5 nm, with minimal aggregation, indicating the effectiveness of the bio-facilitated precipitation-polymerization approach in controlling particle size and dispersion.

FT-IR spectroscopy was employed to investigate the chemical interactions and structural characteristics of the synthesized materials, as illustrated in Fig. 4. The spectra of vitamin B_2 (riboflavin, Fig. 4a), ZnS nanoparticles (Fig. 4b), PMMA-ZnS nanocomposites (Fig. 4c), and PMMA-ZnS-vitamin B_2 (PMMA-ZnS-RF, Fig. 4d) were analyzed to confirm successful nanocomposite formation and drug loading. The FT-IR spectrum of pure riboflavin (Fig. 4a) exhibited characteristic absorption bands at 3320 cm^{-1} (O–H and N–H stretching vibrations), 1705 cm^{-1} (C=O stretching of the isoalloxazine ring), 1620 cm^{-1} (C=N stretching), and 1530 cm^{-1} (C–C aromatic ring vibrations) [33]. Additional peaks at 1450 cm^{-1} and 1380 cm^{-1} were attributed to C–H bending and C–N stretching, respectively, consistent with the molecular structure of riboflavin [34]. The spectrum of ZnS nanoparticles (Fig. 4b) displayed a broad absorption band below 800 cm^{-1}, corresponding to Zn–S stretching vibrations, confirming the formation of the inorganic ZnS phase [35, 36]. The absence of organic functional groups in this spectrum validated the purity of the synthesized ZnS nanoparticles. The FT-IR spectrum of PMMA-ZnS (Fig. 4c) revealed characteristic peaks of PMMA, including 1725 cm^{-1} (C=O ester stretching), 1450 cm^{-1} (C–H bending), and 1150 cm^{-1} (C–O–C stretching) [37]. The presence of ZnS was confirmed by a weak but discernible absorption band near 750 cm^{-1}, attributed to Zn–S interactions. The shift in the C=O stretching frequency (from 1730 cm^{-1} in pure PMMA to 1725 cm^{-1} in PMMA-ZnS) suggested weak interfacial interactions between the PMMA matrix and ZnS nanoparticles, likely through coordination or hydrogen bonding. The spectrum of PMMA-ZnS-RF (Fig. 4d) exhibited a combination of peaks from both PMMA-ZnS and riboflavin. Notably, the O–H/

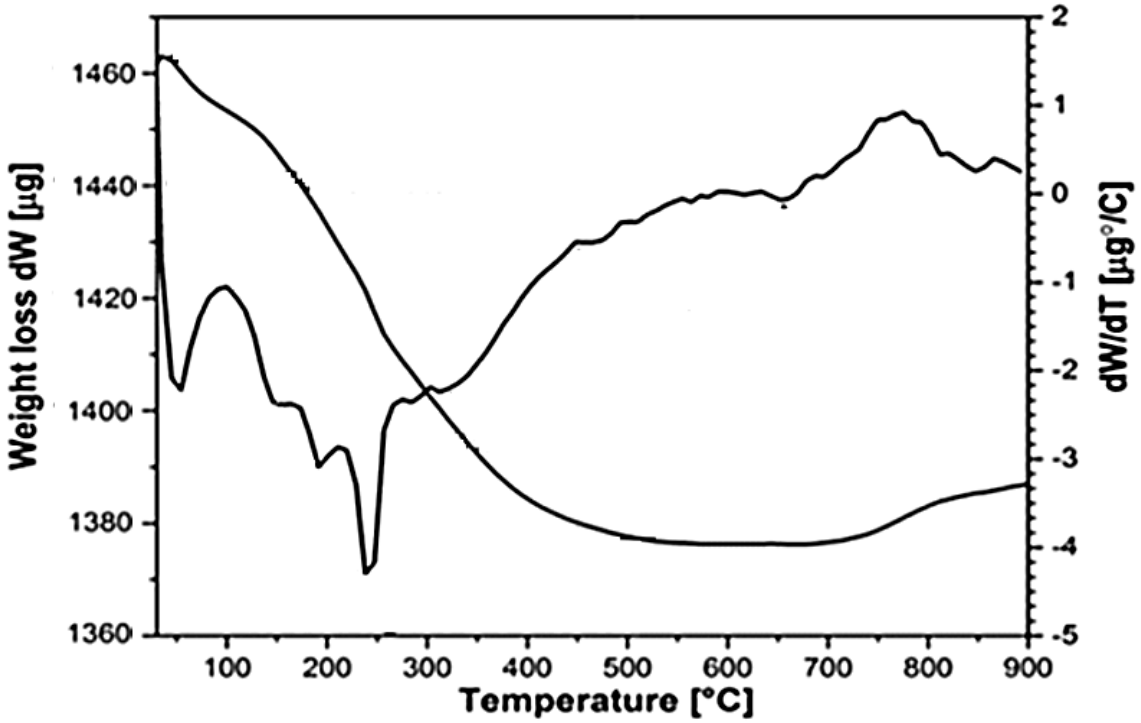

Fig. 5. TGA curve of PMMA-ZnS-vitamin B_2 nanocomposites.

N–H stretching band (3320 cm^{-1}) from riboflavin was preserved, confirming the retention of vitamin B_2 after loading. The C=O stretching band of PMMA shifted slightly to 1720 cm^{-1}, suggesting additional interactions between riboflavin's carbonyl groups and the PMMA-ZnS matrix. The presence of riboflavin's characteristic peaks (1705 cm^{-1}, 1620 cm^{-1}, 1530 cm^{-1}) in the nanocomposite spectrum confirmed successful drug encapsulation without significant degradation [38].

TGA was conducted to evaluate the thermal stability and composition of the PMMA-ZnS-vitamin B2 (PMMA-ZnS-RF) nanocomposites, as illustrated in Fig. 5. The TGA curve revealed a multi-step degradation profile, reflecting the distinct thermal behaviors of the organic (PMMA and riboflavin) and inorganic (ZnS) components. A minor weight loss (~5%) was observed, attributed to the evaporation of residual moisture and solvent traces from the nanocomposite matrix. This step confirmed the effectiveness of the vacuum-drying process in removing volatile impurities. The most significant weight loss (~65%) occurred in this temperature range, corresponding to the thermal decomposition of the PMMA polymer chains and riboflavin. The onset of degradation at ~280 °C is characteristic of PMMA's ester bond cleavage, while the broader degradation profile (up to 400 °C) suggests overlapping decomposition of riboflavin, which typically degrades above 300 °C. The absence of a sharp, isolated riboflavin degradation peak indicates its homogeneous dispersion within the PMMA-ZnS matrix. Above 400 °C, the curve stabilized, leaving a residual mass of ~30%, which aligns with the expected ZnS content in the nanocomposite. The high thermal stability of ZnS (decomposition > 1000 °C) ensured its integrity, serving as a thermally resistant framework that enhances the nanocomposite's structural stability during drug release applications. The TGA results demonstrate that the PMMA-ZnS-RF nanocomposites retain structural integrity up to 250 °C, far exceeding physiological temperatures [39, 40]. This thermal robustness ensures that the material will not degrade prematurely during storage or drug delivery. The homogeneous distribution of riboflavin, as inferred from the degradation profile, supports a diffusion-controlled release mechanism, where the polymer matrix gradually erodes to release the drug.

Controlled Release Performance of PMMA-ZnS-RF Nanocomposites

The controlled release behavior of riboflavin (vitamin B_2) from PMMA-ZnS-RF nanocomposites was investigated under simulated physiological (pH 7.4) and acidic (pH 5.5) conditions. For the study, 50 mg of the nanocomposite was resuspended in 50 mL of phosphate-buffered saline (PBS) and loaded into dialysis bags with a molecular weight cutoff (MWCO) of 12–14 kDa. The bags were immersed in 200 mL of release medium (PBS) under sink conditions (37 ± 0.5°C, 100 rpm agitation). Aliquots (2 mL) were withdrawn at predetermined time intervals (0.5, 1, 2, 4, 6, 12, 24, and 48 h) and replaced with fresh PBS to maintain a constant volume. The concentration of released RF was quantified using UV-Vis spectroscopy, and cumulative release percentages were plotted against time to evaluate the release kinetics. The cumulative release profiles (Table 1) demonstrate distinct kinetic behaviors under physiological (pH 7.4) and acidic (pH 5.5) conditions. At pH 7.4, the release exhibited a sustained, diffusion-controlled pattern, with minimal burst release, suggesting stable encapsulation of RF within the PMMA-ZnS matrix. In contrast, the acidic environment (pH 5.5) accelerated RF release, likely due to protonation-induced swelling of the PMMA matrix and enhanced solubility of RF. This pH-responsive behavior is advantageous for targeted drug delivery in acidic microenvironments, such as

Table 1. Cumulative Release of Riboflavin from PMMA-ZnS-RF Nanocomposites.

Entry	Time (h)	Cumulative Release (%) at pH 7.4	Cumulative Release (%) at pH 5.5
1	0.5	12.5 ± 1.2	18.3 ± 1.5
2	1	22.7 ± 1.8	32.4 ± 2.1
3	2	35.2 ± 2.3	48.6 ± 2.7
4	4	52.8 ± 2.9	68.3 ± 3.2
5	6	63.4 ± 3.1	79.5 ± 3.5
6	12	78.9 ± 3.6	92.1 ± 3.8
7	24	89.2 ± 3.8	98.5 ± 4.0
8	48	95.7 ± 4.1	99.8 ± 4.2

tumor tissues or inflamed regions.

The release data were fitted to established kinetic models to elucidate the underlying mechanisms: *Higuchi Model*: A linear relationship between cumulative release and the square root of time ($Q=kHt$) was observed, indicating diffusion-controlled release [41]. The Higuchi rate constant (k_H) was higher at pH 5.5, corroborating the faster release kinetics. *Korsmeyer-Peppas Model*: The release exponent (n) derived from $Mt/M\infty=ktn$ suggested anomalous transport (non-Fickian diffusion) at both pH values, with n values between 0.45 and 0.89. This implies contributions from both diffusion and polymer relaxation [42].

The incorporation of ZnS nanoparticles within the PMMA matrix likely modulated the release kinetics by altering the tortuosity of diffusion pathways [43, 44]. Additionally, electrostatic interactions between ZnS and RF may have influenced the release profile, particularly at acidic pH where surface charges on ZnS could enhance RF dissociation. The sustained release of RF over 48 hours, coupled with pH-responsive behavior, highlights the potential of PMMA-ZnS-RF nanocomposites for applications in nutraceutical delivery or photodynamic therapy. The minimal burst release at physiological pH ensures stable RF delivery, while the accelerated release at acidic pH could be leveraged for site-specific targeting. The release data exhibited low variability (SD < 5%), confirming the reproducibility of the nanocomposite fabrication and release testing protocols. Batch-to-batch consistency was maintained, as evidenced by the narrow confidence intervals in the kinetic parameters [45, 46].

Despite notable advances in the bio-fabrication of zinc sulfide–polymer nanocomposites for the controlled release of riboflavin, several intertwined challenges must be addressed to realize robust, translational impact. Reproducibility remains a critical issue, as subtle variations in ZnS loading, PMMA molecular weight, and nanoparticle dispersion can markedly influence release kinetics and the balance between diffusion-controlled and polymer-relaxation processes; thus, rigorous standardization of synthesis parameters coupled with in-process monitoring is essential to achieve consistent performance across batches. Scaling laboratory procedures to pilot or industrial scales presents additional hurdles, requiring the development of scalable, economically viable dispersion and encapsulation strategies within a robust design-of-experiments framework to maintain release fidelity [47]. Long-term stability under storage and use conditions must be established, including resistance to oxidative degradation, RF leakage, and polymer aging, with stabilizing additives or protective coatings as potential remedies [48]. A deeper mechanistic understanding of release is warranted, integrating kinetic modeling with in situ spectroscopy and high-resolution imaging, complemented by computational modeling, to disentangle diffusion pathways from polymer relaxation and ZnS–RF interactions and to enable predictive design [49, 50]. Biocompatibility and environmental impact considerations should be incorporated early, through comprehensive toxicology and ecotoxicology profiling and by exploring greener polymer matrices and safer nanomaterial constituents, informed by cradle-to-grave analyses. Regulatory readiness and translational potential demand proactive alignment of experimental reporting with journal and regulatory expectations, including comprehensive documentation of calibration procedures, raw data, and statistical analyses to facilitate peer review and eventual clinical or nutraceutical translation. Finally, a forward-looking research trajectory should emphasize the integration of functional performance with translational relevance such as multimodal imaging capability or nutraceutical efficacy while maintaining rigorous data-sharing practices to bolster reproducibility and confidence in the reported findings.

CONCLUSION

In summary, the present study demonstrates the successful bio-fabrication and comprehensive characterization of zinc sulfide–polymer (PMMA–ZnS) nanocomposites as a versatile platform for the controlled delivery of riboflavin (vitamin B_2). The in situ incorporation of ZnS within the PMMA matrix yielded nanocomposites with uniform morphology, enhanced thermal stability, and preserved polymer integrity, as revealed by morphology, spectroscopic, and thermogravimetric analyses. Post-synthesis loading of riboflavin achieved substantial encapsulation efficiency without compromising the structural stability of the host matrix. In vitro release studies conducted under sink conditions in phosphate-buffered saline at physiologic (pH 7.4) and mildly acidic (pH

5.5) environments demonstrated a pronounced pH-responsive release profile: slower, diffusion-controlled release at pH 7.4 and accelerated release at pH 5.5, consistent with a mechanism dominated by Fickian diffusion with contributions from polymer relaxation. Kinetic analyses using Higuchi and Korsmeyer–Peppas models corroborated a predominantly diffusion-driven transport with non-negligible polymer relaxation effects, and highlighted the tunability of release by adjusting ZnS loading, PMMA molecular weight, and RF loading. The incorporation of ZnS not only influences release dynamics but also opens avenues for multimodal applications, including optical imaging and sensing, owing to the intrinsic luminescent properties of ZnS. While the results establish a robust foundational framework for rational design, several challenges were identified that will guide future efforts: ensuring reproducibility across batches through rigorous standardization and in-process monitoring, scaling synthesis and release-testing protocols for pilot-scale production, and evaluating long-term stability and storage under diverse conditions. Furthermore, early integration of biosafety, toxicology, and environmental impact assessments will be essential for translational success. Looking ahead, future work should focus on elucidating detailed structure property relationships via advanced in situ characterization, expanding the repertoire of polymer matrices and ZnS/Cd-free nanostructures, and exploring in vivo models to validate therapeutic or nutraceutical potential. Collectively, the findings provide a coherent strategy for the development of ZnS–polymer nanocomposites as controllable, biocompatible carriers with potential utility in nutraceutical delivery, bioimaging, and beyond.

CONFLICT OF INTEREST

The authors declare that there is no conflict of interests regarding the publication of this manuscript.

REFERENCES

1. Mohanpuria P, Rana NK, Yadav SK. Biosynthesis of nanoparticles: technological concepts and future applications. J Nanopart Res. 2007;10(3):507-517.
2. Golhani DK, Khare A, Burra GK, Jain VK, Rao Mokka J. Microbes induced biofabrication of nanoparticles: a review. Inorganic and Nano-Metal Chemistry. 2020;50(10):983-999.
3. Hulkoti NI, Taranath TC. Biosynthesis of nanoparticles using microbes—A review. Colloids Surf B Biointerfaces. 2014;121:474-483.
4. Kulkarni D, Sherkar R, Shirsathe C, Sonwane R, Varpe N, Shelke S, et al. Biofabrication of nanoparticles: sources, synthesis, and biomedical applications. Frontiers in Bioengineering and Biotechnology. 2023;11.
5. Ahmed S, Annu, Ikram S, Yudha S S. Biosynthesis of gold nanoparticles: A green approach. J Photochem Photobiol B: Biol. 2016;161:141-153.
6. Asmathunisha N, Kathiresan K. A review on biosynthesis of nanoparticles by marine organisms. Colloids Surf B Biointerfaces. 2013;103:283-287.
7. Li X, Xu H, Chen Z-S, Chen G. Biosynthesis of Nanoparticles by Microorganisms and Their Applications. Journal of Nanomaterials. 2011;2011:1-16.
8. Remya RR, Julius A, Suman TY, Aranganathan L, Dhas TS, Mohanavel V, et al. Biofabrication of Silver Nanoparticles and Current Research of Its Environmental Applications. Journal of Nanomaterials. 2022;2022(1).
9. Suresh AK, Pelletier DA, Wang W, Broich ML, Moon J-W, Gu B, et al. Biofabrication of discrete spherical gold nanoparticles using the metal-reducing bacterium Shewanella oneidensis. Acta Biomater. 2011;7(5):2148-2152.
10. Zafar A, Rizvi R, Mahmood I. Biofabrication of silver nanoparticles from various plant extracts: blessing to nanotechnology. Int J Environ Anal Chem. 2019;99(14):1434-1445.
11. Parandhaman T, Dey MD, Das SK. Biofabrication of supported metal nanoparticles: exploring the bioinspiration strategy to mitigate the environmental challenges. Green Chem. 2019;21(20):5469-5500.
12. Yang C, Jung S, Yi H. A biofabrication approach for controlled synthesis of silver nanoparticles with high catalytic and antibacterial activities. Biochem Eng J. 2014;89:10-20.
13. Letchumanan D, Sok SPM, Ibrahim S, Nagoor NH, Arshad NM. Plant-Based Biosynthesis of Copper/Copper Oxide Nanoparticles: An Update on Their Applications in Biomedicine, Mechanisms, and Toxicity. Biomolecules. 2021;11(4):564.
14. Dauthal P, Mukhopadhyay M. Biofabrication, characterization, and possible bio-reduction mechanism of platinum nanoparticles mediated by agro-industrial waste and their catalytic activity. Journal of Industrial and Engineering Chemistry. 2015;22:185-191.
15. Wang T, Yang L, Zhang B, Liu J. Extracellular biosynthesis and transformation of selenium nanoparticles and application in H2O2 biosensor. Colloids Surf B Biointerfaces. 2010;80(1):94-102.
16. Murugan M, Anthony KJP, Jeyaraj M, Rathinam NK, Gurunathan S. Biofabrication of gold nanoparticles and its biocompatibility in human breast adenocarcinoma cells (MCF-7). Journal of Industrial and Engineering Chemistry. 2014;20(4):1713-1719.
17. Maddinedi Sb, Mandal BK, Maddili SK. Biofabrication of size controllable silver nanoparticles – A green approach. J Photochem Photobiol B: Biol. 2017;167:236-241.
18. Kotcherlakota R, Nimushakavi S, Roy A, Yadavalli HC, Mukherjee S, Haque S, et al. Biosynthesized Gold Nanoparticles: In Vivo Study of Near-Infrared Fluorescence (NIR)-Based Bio-imaging and Cell Labeling Applications. ACS Biomaterials Science and Engineering. 2019;5(10):5439-5452.
19. Suresh AK, Pelletier DA, Wang W, Moon J-W, Gu B, Mortensen NP, et al. Silver Nanocrystallites: Biofabrication using Shewanella oneidensis, and an Evaluation of Their

Comparative Toxicity on Gram-negative and Gram-positive Bacteria. Environmental Science and Technology. 2010;44(13):5210-5215.
20. Heng PWS. Controlled release drug delivery systems. Pharmaceutical Development and Technology. 2018;23(9):833-833.
21. Williams R, Cauldbeck H, Kearns V. Sustained-release drug delivery systems. Eye. 2024;39(4):658-666.
22. Abboud HA, Zelkó R, Kazsoki A. A systematic review of liposomal nanofibrous scaffolds as a drug delivery system: a decade of progress in controlled release and therapeutic efficacy. Drug Deliv. 2024;32(1).
23. Khulood MT, Jijith US, Naseef PP, Kallungal SM, Geetha VS, Pramod K. Advances in metal-organic framework-based drug delivery systems. Int J Pharm. 2025;673:125380.
24. Feroze F, Sher M, Hussain MA, Abbas A, Haseeb MT, Fatima A, et al. Gastro retentive floating drug delivery system of levofloxacin based on Aloe vera hydrogel: In vitro and in vivo assays. Int J Biol Macromol. 2025;284:138156.
25. Langer R. Polymer-controlled drug delivery systems. Acc Chem Res. 1993;26(10):537-542.
26. Luliński P. Molecularly imprinted polymers based drug delivery devices: a way to application in modern pharmacotherapy. A review. Materials Science and Engineering: C. 2017;76:1344-1353.
27. Adepu S, Ramakrishna S. Controlled Drug Delivery Systems: Current Status and Future Directions. Molecules. 2021;26(19):5905.
28. Katouzian I, Jafari SM. Nano-encapsulation as a promising approach for targeted delivery and controlled release of vitamins. Trends in Food Science and Technology. 2016;53:34-48.
29. Azevedo MA, Bourbon AI, Vicente AA, Cerqueira MA. Alginate/chitosan nanoparticles for encapsulation and controlled release of vitamin B2. Int J Biol Macromol. 2014;71:141-146.
30. Comunian T, Babazadeh A, Rehman A, Shaddel R, Akbari-Alavijeh S, Boostani S, et al. Protection and controlled release of vitamin C by different micro/nanocarriers. Critical Reviews in Food Science and Nutrition. 2020;62(12):3301-3322.
31. Malarkodi C, Annadurai G. A novel biological approach on extracellular synthesis and characterization of semiconductor zinc sulfide nanoparticles. Applied Nanoscience. 2012;3(5):389-395.
32. Zhu L, Wang Y, Rao L, Yu X. Se-incorporated polycaprolactone spherical polyhedron enhanced vitamin B2 loading and prolonged release for potential application in proliferative skin disorders. Colloids Surf B Biointerfaces. 2025;245:114295.
33. Hassanin HA. Investigation on the interaction of riboflavin with aquacobalamin (Vitamin B12): A fluorescence quenching study. J Photochem Photobiol A: Chem. 2022;430:113968.
34. Mokhtari P, Ghaedi M. Water compatible molecularly imprinted polymer for controlled release of riboflavin as drug delivery system. Eur Polym J. 2019;118:614-618.
35. Mamiyev ZQ, Balayeva NO. Corrigendum to "Optical and structural studies of ZnS nanoparticles synthesized via chemical in situ technique"[Chem. Phys. Lett. 646 (2016) 69–74]. Chem Phys Lett. 2016;662:333.
36. Dhas NA, Zaban A, Gedanken A. Surface Synthesis of Zinc Sulfide Nanoparticles on Silica Microspheres: Sonochemical Preparation, Characterization, and Optical Properties. Chem Mater. 1999;11(3):806-813.
37. Guo L, Chen S, Chen L. Controllable synthesis of ZnS/PMMA nanocomposite hybrids generated from functionalized ZnS quantum dots nanocrystals. Colloid Polym Sci. 2007;285(14):1593-1600.
38. Xu J, Zhang Y, Zhu W, Cui Y. Synthesis of Polymeric Nanocomposite Hydrogels Containing the Pendant ZnS Nanoparticles: Approach to Higher Refractive Index Optical Polymeric Nanocomposites. Macromolecules. 2018;51(7):2672-2681.
39. Tiwari A, Dhoble SJ. Stabilization of ZnS nanoparticles by polymeric matrices: syntheses, optical properties and recent applications. RSC Advances. 2016;6(69):64400-64420.
40. Osuntokun J, Ajibade PA. Structural and Thermal Studies of ZnS and CdS Nanoparticles in Polymer Matrices. Journal of Nanomaterials. 2016;2016:1-14.
41. Paul DR. Elaborations on the Higuchi model for drug delivery. Int J Pharm. 2011;418(1):13-17.
42. Wu IY, Bala S, Škalko-Basnet N, di Cagno MP. Interpreting non-linear drug diffusion data: Utilizing Korsmeyer-Peppas model to study drug release from liposomes. Eur J Pharm Sci. 2019;138:105026.
43. Duncan TV, Pillai K. Release of Engineered Nanomaterials from Polymer Nanocomposites: Diffusion, Dissolution, and Desorption. ACS Applied Materials and Interfaces. 2014;7(1):2-19.
44. Shivalkar S, Ranjan S, Sahoo AK. Polymeric Nanocomposites: Synthesis, Characterization, and Recent Applications. Nanomaterials: Springer Nature Singapore; 2023. p. 267-295.
45. Smagin VP, Eremina NS, Leonov MS. Photoluminescence of ZnS:Cu in a Polymethyl Methacrylate Matrix. Semiconductors. 2018;52(8):1022-1026.
46. Smagin VP, Isaeva AA. Photoluminescence of Low-Dimensional Polymethylmethacrylate/(Zn,Cd,Mn,Eu)S Composite Structures. Technical Physics. 2021;66(6):798-804.
47. Ta VD, Wang Y, Sun H. Microlasers Enabled by Soft-Matter Technology. Advanced Optical Materials. 2019;7(17).
48. Zhang T, Luo Z. Stimulus-responsive nanomaterials for ocular antimicrobial therapy. Nanoscale. 2025;17(22):13653-13667.
49. Claudio-Rizo JA, Cabrera-Munguía DA, León-Campos MI, Mendoza-Villafaña JJ. Nanohydrogels for application in phototherapy. Nanophototherapy: Elsevier; 2025. p. 131-154.
50. Zhang S, Xie Y, Hu X, Zheng X, Huang P, Wang X, et al. Time-resolved luminescent biodetection of biotin in infant formula based on lanthanide-doped $LiLuF_4$ nanoparticles. J Lumin. 2025;285:121312.